
LOW-RANK INTERCONNECTED ADAPTATION ACROSS LAYERS

Yibo Zhong
Sichuan University
Chengdu, China
zhongyibo@stu.scu.edu.cn

Yao Zhou*
Sichuan University
Chengdu, China
yaozhou@scu.edu.cn

ABSTRACT

Low-rank adaptation (LoRA), as one of the most well-known representative method of parameter-efficient fine-tuning, freezes the backbone model and introduce parallel adapter modules to each layer of the model. These modules consist of two low-rank trainable matrices: a low-dimension projector (LP) and a high-dimension projector (HP) with their product approximating the change for updating the model weight. However, the LP and HP for each layer are paired, and the input fed into the corresponding LP immediately goes into the paired HP for that particular layer. This setup constrains the learned ΔW to the current layer and therefore a particular level of features, as models like Transformers are composed of many stacked layers, each extracting information at different levels. By considering the differences between layers and establishing connections across them when learning ΔW , we enhance the capture of relevant information for downstream tasks using this interconnected adaptation when fine-tuning. Meanwhile, preserving the unique characteristics of each layer and thus selectively mix the learning traits of various layers according to a specific ratio can also be crucial in certain tasks. In this paper, we propose Low-rank interconnected adaptation across layers (Lily). Specifically, to liberate the projection matrices in LoRA from their layer-specific constraints, we employ a hierarchical strategy where we retain the LPs at the layer level, tasked with projecting distinct layer features to a low dimension, dubbed local LP. Conversely, we detach all HPs from their respective layers, transforming them into a model-shared module named global HP. Owing to its layer independence, the global HP accommodates any number of HP sub-modules or, drawing inspiration from mixture of experts (MoE), multiple HP experts that transcend layer positions while capturing learning traits across diverse layer categories from shallow to deep. For the ratio to mix all the experts, we use a router inspired by MoE to selectively adapt the features of different layers, thus obtaining a unique expert distribution. We evaluated Lily on a wide range of downstream tasks and achieved state-of-the-art results, outperforming LoRA and a range of competitive methods. Code will be available at Github.

1 Introduction

For foundation models like the Transformer [26], fine-tuning them on downstream tasks is a typical use case. However, direct fine-tuning (also known as full fine-tuning or FFT) comes with a host of issues, including huge computational and storage costs when dealing with large models, as well as the risk of forgetting previously learned knowledge [4]. While fine-tuning only the final module, such as the classification head (a technique known as linear probing), addresses these problems, it leads to a significant degradation in performance. To tackle these challenges, the research community has paid significant attention to Parameter-Efficient Transfer Learning (PETL). In PETL, the given model is used as a backbone and its weights are frozen. Instead of modifying the entire model, lightweight trainable modules called adapters are introduced to efficiently learn the changes in the backbone weights. We denote the frozen weights in the backbone as W , and the learned task-specific incremental weight updates as ΔW . Among the various PETL methods, Low-rank Adaptation (LoRA [14]) is one of the most well-known and widely applied techniques. LoRA introduces a pair of adapter modules in each layer of the model, consisting of two projection matrices. One matrix, the low-dimension projector (LP), projects the input x to a low-dimension form, while the other, the high-dimension projector, restores the low-dimension representation back to its original dimension. By multiplying these two projection matrices, we can approximate the actual ΔW in full fine-tuning. Additionally, since both projection matrices are

low-rank, LoRA offers significant savings in computational and storage costs, effectively alleviating the burdens of full fine-tuning. Moreover, by specifically learning the ΔW for the downstream task, LoRA could outperform linear probing by a considerable margin.

However, LoRA and many subsequent improvements to the method [19] [31] [32] are limited by a specific setting introduced by it: the LP and its corresponding HP always appear as a pair in the same layer. In other words, when the input x is projected to a low-rank subspace by the LP, it is immediately fed into the paired HP in the same layer. This limitation arises because models like the Transformer, which are composed of multiple stacked layers, exhibit varying characteristics in feature learning and extraction across different layers [27]. Restricting the learning of ΔW to the current layer ignores the knowledge and features learned in other layers, which could be potentially beneficial to the adaptation. Many Prior models have already been designed with cross-layer connections to better associate different layers. For example, the skip-connection in UNet [22] merges the features of the lower and higher layers for learning. Another example is UNet++ [33], which is a typical representative of cross-layer feature fusion. The design of these models offers an important insight: connecting the layers of a deep learning model can potentially lead to a more comprehensive understanding of the task. Therefore, we believe that this intuition is not only useful in model architecture design but also applicable to the adaptation process. To this end, we design a method that takes into account information from all layers when dealing with features at different levels via a hierarchical structure, namely interconnected adaptation, thus resulting in a more comprehensive and holistic approach to feature extraction and the learning of ΔW .

However, it is not enough to simply incorporate information from all other layers. It is also important to preserve the unique features of each layer and selectively combine information from different layers. Inspired by self-attention, which calculates the relationship between each token and all other tokens and obtains attention scores indicating the strength of the relationship, we also selectively incorporate the weight of different layers based on their relationship with the current layer we focus on. Due to the widespread use of MoE [23] techniques in various fields, we employ an MoE router to achieve the effect of selective combination.

In this paper, we propose **Low-rank interconnected adaptation across layers (Lily)**, a self attention inspired low-rank adaptation method for PETL. Specifically, we set a local LP in each layer to project the input x to a low-dimensional space. Then, x is passed to the global HP, whose router selectively outputs an expert distribution to combine the outputs of different HP experts, each specializing in feature learning for a specific layer. By doing so, we can take into account information from all layers during adaptation at each level and achieve a selective property across layers, similar to self-attention. This comprehensive perspective enhances our adaptation performance. Our contributions are as follows:

- We propose a novel generic framework for low-rank adaptation, named **Low-rank interconnected adaptation across layers (Lily)**. Lily goes beyond adapting to the current layer and takes into account information from all the layers in the model, providing a more comprehensive understanding during adaptation.
- A hierarchical adaptation structure is designed: LPs at the local level, capturing layer-specific information, and HPs at the global level, helping adaptation to take into account information from all other layers. This hierarchy can provide a more flexible configuration and ultimately achieve better performance with fewer parameters.

2 Related Work

2.1 Foundation Models

The Transformer architecture has emerged as the most widely adopted model structure, finding applications in various industrial contexts. At the heart of the Transformer lies the self-attention mechanism [26], a powerful tool for modeling relationships and dependencies. By computing weights for the current token relative to all other tokens in the sequence and producing a weighted sum, self-attention ensures that the processing of each token takes into account its relationship with all other tokens.

Recently many models are proposed trying to challenge Transformer as the potential next generation foundation model including [11] [20] [2]. Among these challengers, Mamba [11] is a type of architecture that gains much focus, built on structured state space models (S4). S4, related to RNNs [12] and CNNs [17], is defined by parameters (Δ, A, B, C) . Through discretization, S4 derives (\bar{A}, \bar{B}, C) from these parameters. S4 updates hidden states and generates outputs using these derived parameters, with the unique ability to do so via recurrence or global convolution. Mamba enhances S4 by introducing a selective property and proposes a hardware-aware algorithm, effectively addressing parallel training challenges.

Both Transformers and their emerging challengers share a common trait: they are composed of multiple stacked layers. Many models, such as UNet [22] and UNet++ [33], have recognized that linking layers of different levels through techniques like skip-connections can better capture features, and they have achieved excellent results and wide applications. Therefore, it is beneficial to consider the information of all other layers together with the current layer during both the pre-training and adaptation processes.

2.2 Parameter Efficient Transfer Learning

Typical usage of Foundation Models includes pre-training on large datasets and fine-tuning or adaptation to various downstream tasks. However, traditional adaptation methods such as full fine-tuning and linear probing have significant drawbacks, including high computation and storage costs or sub-optimal performance, which hinder their widespread adoption when dealing with large models. To address these issues, Parameter-Efficient Transfer Learning (PETL) emerges as a promising field, aiming to adapt the model backbone efficiently with as few parameters as possible while maintaining the performance and knowledge.

Current PETL research is predominantly conducted on Transformer architecture due to its popularity and can be mainly categorized into two types: 1) adapter-based methods [14] [5] [21] [15] [13] and 2) prompt-based methods [24] [25]. Adapter-based methods introduce lightweight adapters into the Multi-Head Self-Attention (MHSA) or the Feed-Forward Network (FFN) blocks within the Transformer architecture. On the other hand, prompt-based methods append trainable tokens as prompts to the input tokens fed to the network.

Among the various PETL techniques, Low-rank Adaptation (LoRA) stands out as the most well-known method. LoRA introduces a pair of adapter modules per layer, each comprising two projection matrices. The low-dimension projector (LP) converts input x to low-dimension form, and the high-dimension projector (HP) restores it to the original dimension. Multiplying these projections approximates the ΔW in full fine-tuning.

However, LoRA has limitations, one of which is that its LP and HP always appear as pairs in each layer. As a result, the information they receive and the ΔW they learn are confined to the current layer. As discussed in the previous section, incorporating information from all other layers during the adaptation can address this limitation and this is precisely why Lily detaches the HPs from the layers.

2.3 Mixture of Experts

Mixture of Experts (MoE) is an active research area that has garnered significant attention especially in the field of Large Language Models (LLMs). Conditional computation, where different parts of the network are activated on a per-example basis, has been proposed to enhance model capability without increasing computation [6] [3] [9] [1]. The Sparsely-Gated Mixture-of-Experts (MoE) layer is introduced to implement this idea, consisting of numerous sub-networks [23]. A trainable gating network, known as a "router", determines the combination of experts for each example, which can be a soft routing approach using a weighted sum of all experts or discrete routing with sparse weights [23]. There're already PETL methods like MoLORA [29] and MOLA [10] which apply the MoE design concept to PETL. However, these methods simply treat the LP and HP combined in LoRA as a single expert, still positioned at layer-specific locations. A concurrent research [28], utilizes the LP and HP sub-spaces as experts but fails to overcome the limitation in previous section: when LP and HP appear in pairs in the same layer, the learned ΔW is limited to that layer without an understanding of information from all other layers.

3 Method

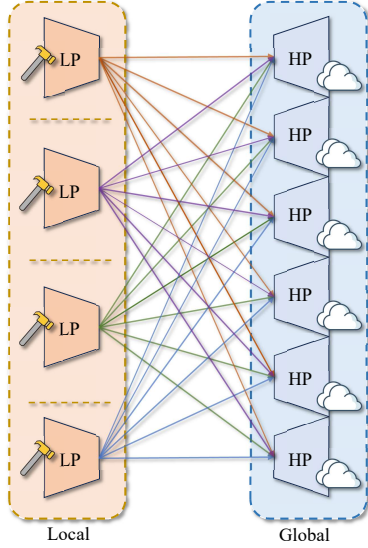
We introduce **Low-rank interconnected adaptation across layers (Lily)** in this section. Initially, the specific model architecture utilized is detailed, followed by an explanation of the overall adaptation process. Subsequently, we present Lily on two distinct models, the Transformer and Mamba, to validate its versatility.

3.1 Overview of Lily

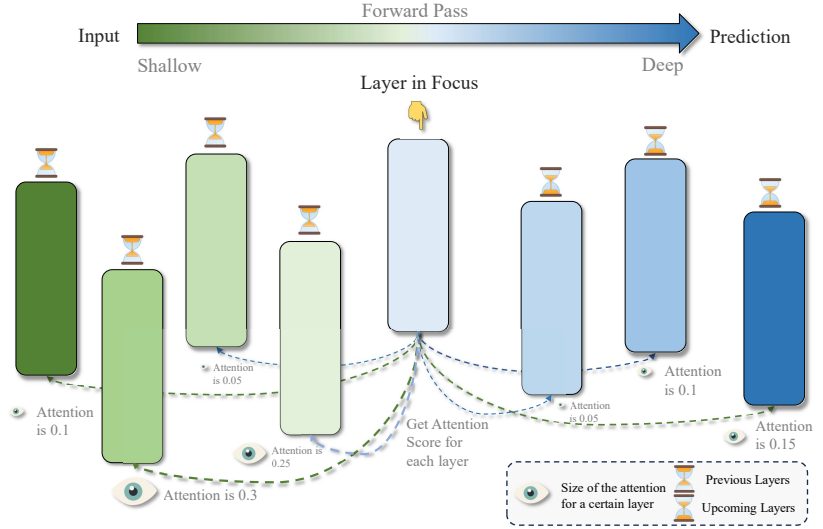
To begin with, the computation process of Low-rank Adaptation (LoRA) can be expressed as follows when setting the rank to d :

$$W' = W + P_L P_H \tag{1}$$

where $W \in \mathbb{R}^{a \times b}$ is the frozen weight in the backbone, and $P_L \in \mathbb{R}^{a \times d}$ and $P_H \in \mathbb{R}^{d \times b}$ are the low-dimension projectors (LPs) and the high-dimension projectors (HPs). Therefore, during the training process the forward propagation



(a) Illustration of the hierarchical structure of Lily: Specifically, all the LPs are pinned to specific types of layers at the bottom of the hierarchy, while all the HPs are detached from the layers, sitting at the top of the hierarchy.



(b) An example of the adaptive nature of Lily. Here we choose one specific layer as the current focus during the forward propagation. Using a router, we could calculate the relativity scores between the current layer and all the other layers and use these scores as the weights of the HP experts.

Figure 1: Structure and adaptive nature of Lily.

can be described as:

$$\begin{aligned}
 x' &= xP_L && \leftarrow \text{(low-dimension projection)} \\
 x' &= x'P_H && \leftarrow \text{(extra knowledge)} \\
 x &= xW && \leftarrow \text{(basic knowledge)} \\
 x &= x + x' &&
 \end{aligned} \tag{2}$$

where we denote the output of feeding x to W as the basic knowledge which the backbone model already have, while the output of x transformed by being first projected to low-dimension by P_L and then restored to its original dimension by P_H as extra knowledge which belongs to the current downstream task. In this case, the product of P_L and P_H can approximate ΔW , representing the learned task-specific incremental weight, or extra knowledge.

However, this setup has a limitation: after x is projected through P_L , it is immediately fed into the corresponding paired P_H in the same layer, returning to its original dimension. In this process, the ΔW approximated by P_L and P_H restricts the acquisition of extra knowledge solely to the features of the current layer, limiting its scope to the fixed and predetermined layer. Therefore, inspired by model architectures with cross-layer connections, we believe that when learning the ΔW for the layer of interest, taking into account the information from all other layers is beneficial to the task. However, the layer-specific nature of LoRA falls short in this regard. The model structure of Lily is presented in Fig. 1a. Specifically, to address this limitation, we first decouple the HPs from the layers, setting them free from a fixed position. These HPs now form a group of HP experts, organized as a globally shared module across the entire model, which could be denoted as $P_H^i, i \in \{1, 2, \dots, N_e\}$ where N_e indicating how many HP experts are in this global HP. These experts are expected to each specialize in learning features from a particular level of layers from shallow to deep in the model.

At the same time, to provide layer-specific features for analysis by the global HP and to determine the weights of different experts selectively, we still fix the LPs $P_L^i, i \in \{1, 2, \dots, N_l\}$ in each layer to continuously extract layer-specific features where N_l is the number of layers in the model. This hierarchical structure consists of local LPs at the bottom, which are non-selective and only project the input x of a specific layer into a low-dimensional space, thus extracting layer-specific features. In contrast, the global HP sits at the top of the hierarchy, exhibiting selectivity. It receives the low-dimensional features projected by the local LPs and selectively assigns unique weights to different HP experts, combining information from various layers according to specific ratios. This structure is illustrated in Fig. 1a.

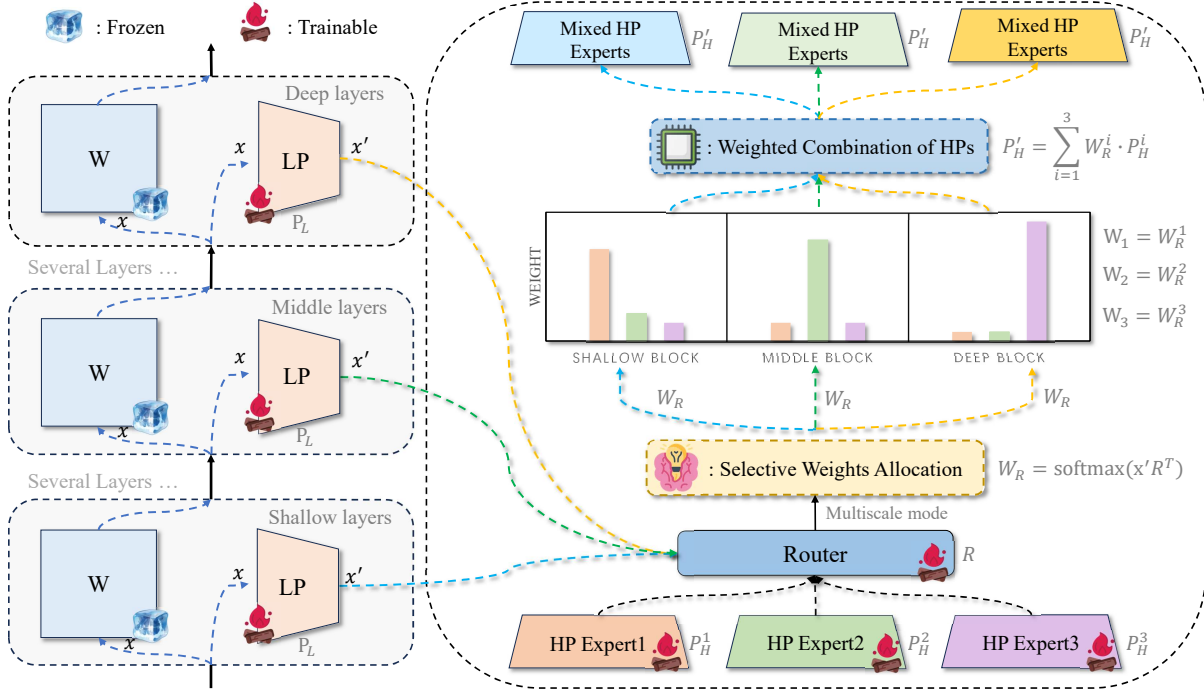


Figure 2: An overview of the whole process of selective weights allocation by the router according to features from layers of different levels: shallow, deep, etc. Following is a weighted combination of all the HP experts to get a final mixed HP for adaptation. The example here we use $N_e = 3$.

Fig. 2 provides a visual guide to the process. To selectively assign weights to different experts, we draw inspiration from the Mixture of Experts (MoE) paradigm and employ a router, $R \in \mathbb{R}^{N_e \times d}$, which transforms the corresponding input into the desired weights. This can be expressed as:

$$\begin{aligned} x' &= xP_L \\ W_R &= \text{softmax}(x'R^T) \end{aligned} \quad (3)$$

Once we obtain the routed weights, W_R , we can compute the weighted combination of all the HP experts, which can be expressed as:

$$P_H^i = \sum_{i=1}^{N_e} W_R^i \cdot P_H^i \quad (4)$$

where W_R^i is the i th weight responding to i th HP expert P_H^i . Finally we obtain the P_H^i as the combination of all the experts, and the high-dimension projection is performed by using P_H^i :

$$x' = x'P_H^i \quad (5)$$

An illustration of the intuition of our approach is presented in Fig 1b. The intuition is that each expert can learn how to transform the input for layers of different depths. Meanwhile, the router can selectively combine all the expert outputs based on the current input. For inputs from shallower layers, the router will increase the weights, which we refer as the attention, for experts specializing in shallow-layer transformations, whereas, for deeper inputs, it will concentrate on the experts learning depth-specific input projections.

3.2 Lily on Transformer

Transformer, as the most widely used foundation model in current applications, has a primary mechanism of multi-head self attention (MHSA), which can be specifically expressed as:

$$MHSA(X) = \sum_{i=1}^N \text{softmax} \left(\frac{XW_q^{(i)}(W_k^{(i)})^T X^T}{\sqrt{d_k}} \right) XW_v^{(i)}(W_o^{(i)})^T \quad (6)$$

For each token, MHSA calculates its relationship with all tokens and obtains the corresponding weight ratio, allowing each token to access information from the entire sequence. This is also the inspiration for Lily. In MHSA, Q, K, and V can all be adapted, and the Feed Forward Network (FFN) can be adapted as well. Following prior work like [14], we take W_q and W_v in MHSA as an example, and Lily for adapting the query Q can be expressed as:

$$Q = XW_q + xP_L^q \sum_1^{N_e} softmax(x'R^T)^i \cdot P_H^{q,i} \quad (7)$$

whereas adapting the value V can be expressed as:

$$V = XW_v + xP_L^v \sum_1^{N_e} softmax(x'R^T)^i \cdot P_H^{v,i} \quad (8)$$

where W_q, W_v are the frozen weights from the backbone, P_L^q, P_L^v are LPs of Q and V respectively, and P_H^q, P_H^v are HP experts in the global HP of Q and V, respectively.

3.3 Lily on Mamba

Mamba and Structured State Space Models (SSMs) utilize parameters (Δ, A, B, C) to transform an input sequence $x(t)$ to an output sequence $y(t)$ using a hidden state $h(t)$. The discretization process converts A and B into \bar{A} and \bar{B} , respectively, using the time step size parameter Δ . SSMs, inspired by continuous systems, can be computed similarly to RNNs or in the form of global convolution due to their Linear Time Invariance (LTI) property. Mamba introduces a selective property to SSMs, tying parameters to the current input x_t , which breaks the LTI property and hinders parallel training. To address this, Mamba employs a hardware-aware algorithm, enabling its SSM module to possess the selective property and perform parallel training. To be specific, the discretization process can be expressed as:

$$\begin{aligned} \bar{A} &= exp(\Delta A) \\ \bar{B} &= (\Delta A)^{-1}(exp(\Delta A) - I) \cdot \Delta B \end{aligned} \quad (9)$$

After that, the calculation in Mamba can be expressed as:

$$\begin{aligned} h_t &= \bar{A}h_{t-1} + \bar{B}x_t \\ y_t &= Ch_t \end{aligned} \quad (10)$$

where h_t is the hidden state at time t and x_t is the corresponding input token. Even though Mamba may seem significantly different from Transformers, it is essentially similar to recent works like linear attention [16], which approximate self-attention instead of directly calculating it to reduce computational complexity. This reveals the deep impact of the self-attention mechanism on sequence modeling.

Since models like Mamba and Transformers are composed of multiple stacked layers, applying Lily to Mamba is quite similar to using it with Transformers. However, just like LoRA focuses on the selection of Q and V, it is important to choose the appropriate positions for adaptation in Mamba. To begin with, Δ is a critical parameter in SSM and therefore Mamba, setting the time step for discretization and indirectly determining parameters \bar{A} and \bar{B} . The discretization process gives \bar{A} and \bar{B} similar functionalities to RNN gates like those in LSTM [12], controlling the hidden state update and influencing output computation. Meanwhile, the linear transformation of the input x at each layer is also crucial, similar to the projection matrix in MHSA. Therefore, we also include these linear transformation matrices denoted as W_{in} as part of our adaptation targets. The whole adaptation process in Lily on Mamba can be expressed as:

$$\begin{aligned} X &= XW_{in} + xP_L^{in} \sum_1^{N_e} softmax(x'R^T)^i \cdot P_H^{in,i} \quad (\text{input adaptation}) \\ \Delta &= XW_{\Delta} + xP_L^{\Delta} \sum_1^{N_e} softmax(x'R^T)^i \cdot P_H^{\Delta,i} \quad (\Delta \text{ adaptation}) \end{aligned} \quad (11)$$

where the W_{in}, W_{Δ} are the frozen weights from the backbone, P_L^{in}, P_L^{Δ} are LPs for the input transformation and the Δ transformation, and P_H^{in}, P_H^{Δ} are HP experts in the global HP adapting input transformation and the Δ transformation.

4 Experiments

4.1 Implementation details

Regarding the choice of the router R , as mentioned earlier, we are inspired by MoE to employ a router that selectively weighs the corresponding experts based on the specific features of the input x . However, unlike the MoE techniques

Algorithm 1 Algorithm for the global HP in PyTorch like pseudo code.

```

1  class mop(nn.Module):
2      """
3      Mixture of dimension Projectors (low or high) (MoP)
4      """
5      def __init__(self, in_dim, out_dim, ne):
6          super().__init__()
7          # router
8          self.router = nn.Linear(in_dim, ne, bias=False)
9          nn.init.normal_(self.router.weight, mean=1.0, std=0.01) # initialize
           with 1s to ensure all the experts have the same share of weight at
           the beginning.
10         # all HP experts
11         self.adapters = nn.Parameter(torch.zeros(ne, in_dim, out_dim))
12
13     def forward(self, x):
14         # get probabilities for all experts and combine them into a single
           adapter
15         # x [B, N, C]
16         router_logits = self.router(x) # [B, N, num_of_experts]
17         router_probability = F.softmax(router_logits, dim=-1) # [B, N, ne]
18         expert_probabilities = router_probability.mean(dim=(0, 1))
19         combined_adapter = torch.einsum("e,eio->io", expert_probabilities,
           self.adapters)
20         return combined_adapter

```

Algorithm 2 An example of Lily on Q transformation in MHSA.

```

1  hidden_q = self.q_lp(x) # Low-dimension x after LP
2  combined_hp_q = self.q_hp(hidden_q) # combination of the HP experts
3  delta_q = torch.einsum("bld,de->ble", hidden_q, combined_hp_q) # Learned
           extra knowledge about the task.

```

commonly used in LLMs, which often involve sparse structures and techniques like gating and top-k selection, we instead use a soft routing approach, as seen in prior work [29]. This means that each expert equally receives the input x and produces an output, and the router determines the weights for combining these outputs. However in the actual implementation, in order to prevent overhead caused by the serial execution of these experts, we combine the experts into one single HP expert and use it to perform the high-dimension projection operation only once. For specific algorithm implementations and usage, please refer to Alg. 1 and Alg. 2.

In many MoE settings, a penalty term is often added to the loss function to prevent certain experts from having consistently high weights while others have negligible weights, or to address situations where the input does not enter the corresponding experts at all [32] [35]. However, in our soft routing approach, this is not only unnecessary but also even undesirable. Firstly, we ensure that all HP experts are considered by combining them. Secondly, the imbalanced weight distributions among experts actually highlight the layer-specific knowledge that has been learned. Adding a penalty term to encourage uniform weight distributions is akin to expecting the experts to aggregate directly, which contradicts the adaptive nature of Lily and negates the role of the router. Therefore, we initialize the weights of the router to 1, ensuring that all experts have equal weights initially, which can also be observed in line 9 of Alg. 1, where in the actual implementation we use a standard normal distribution with a mean of 1.0 to ensure the same initial weights.

4.2 Lily on Transformer

4.2.1 VTAB-1K Benchmark

We evaluate our methods on Visual Task Adaptation Benchmark (VTAB-1K [30]), a suite of visual tasks designed to evaluate general visual representations. The benchmark consists of 19 tasks, spanning a diverse range of domains and semantics. To provide a consistent API for pre-trained models, all tasks are formulated as classification problems.

	Natural							Specialized				Structured							Average	Params(M)	
	Cifar100	Caltech101	DTD	Flowers102	Pets	SVHN	Sun397	Camelyon	EuroSAT	Resisc45	Retinopathy	ClecF-Count	Clevr-Dist	DMLab	KITTI-Dist	dSpr-Loc	dSpr-Ori	sNORB-Azim			sNORB-Ele
<i>Traditional Fine-Tuning</i>																					
Full	68.9	87.7	64.3	97.2	86.9	87.4	38.8	79.7	95.7	84.2	73.9	56.3	58.6	41.7	65.5	57.5	46.7	25.7	29.1	68.9	327
Linear	64.4	85.0	63.2	97.0	86.3	36.6	51.0	78.5	87.5	68.5	74.0	34.3	30.6	33.2	55.4	12.5	20.0	9.6	19.2	57.6	0
<i>PETL methods</i>																					
AdaptFormer	74.0	92.2	71.7	99.3	91.7	88.9	56.4	87.2	95.1	85.7	75.9	84.2	62.2	53.0	81.0	87.1	53.6	35.3	42.3	76.8	0.59
LoRA	72.5	91.5	71.9	99.1	91.4	89.6	56.0	87.6	95.3	84.0	75.0	83.6	64.3	51.6	80.9	86.0	51.8	36.8	42.3	76.4	1.17
<i>Ours</i>																					
Lily (ffn)	74.0	92.6	72.2	99.4	91.5	89.0	55.9	88.2	95.5	85.4	76.0	83.3	62.2	53.0	80.0	86.5	53.8	35.5	43.1	76.8	0.85
Lily (qv)	73.2	92.3	72.2	99.3	91.4	89.0	56.5	87.6	95.2	84.8	75.9	83.7	65.8	52.8	81.2	87.6	52.4	36.3	43.4	76.9	0.78
Lily (qvffn)	73.9	93.2	72.7	99.4	91.6	89.7	56.5	87.9	95.3	85.0	76.0	85.0	65.2	53.0	82.1	86.7	53.0	36.0	42.8	77.1	0.80
Lily (kvffn)	74.1	92.3	72.6	99.3	91.5	89.2	56.7	88.2	95.4	85.3	76.0	84.6	64.9	53.4	81.7	87.5	52.9	36.9	45.2	77.3	0.76

Table 1: Full results of Lily on ViT-B on VTAB-1K benchmark. The average is computed based on the group-wise averages. Green signifies the best performance on the tasks.

The VTAB-1K benchmark is divided by three categories: 1) Natural 2) Specialized 3) Structured. Natural image tasks involve images of the natural world, which are captured by standard cameras, encompassing generic objects, fine-grained classes, or abstract concepts. Specialized tasks, on the other hand, employ images taken with specialized equipment, such as medical or remote sensing imagery. Structured tasks often involve synthetic environments designed to test understanding of specific changes between images, including predicting distances to objects in 3D scenes, counting objects, and detecting orientation.

For the comparison methods, we choose AdaptFormer [5], LoRA [14], as well as traditional fine-tuning methods such as full fine-tuning and linear probing. For Lily, we apply it to different components of ViT, such as W_q , W_v , W_k , and FFN. We denote these settings as qv, qvffn, ffn, and kvffn, respectively, to indicate where Lily is deployed in the model. To ensure a fair comparison, we adjust the rank so that each configuration has the same number of parameters. For qv, we use $d = 32$; for qvffn and kvffn, we use $d = 16$ for the MHSA component and $d = 32$ for FFN. For ffn, we use $d = 64$. The N_e is searched from $\{2, 4, 6, 8\}$ to best adapt to different granularities required for different tasks. Following prior work [15], we use a scaling factor s searched from $\{0.01, 0.1, 1.0, 10.0\}$. As for experimental settings, we use AdamW as the optimizer and a cosine learning-rate scheduler. All the experiments are conducted with a batch size of 64. For the backbone, we use ViT-B/16 [8] pretrained on supervised ImageNet-21K [7].

As the results presented in Table 1, Lily achieves the best performance in 17 out of the 19 tasks in the VTAB-1K benchmark. It can be observed that allocating parameters to different components can lead to significant performance variations across different types of datasets. For instance, Lily (ffn) outperforms other configurations on specialized tasks. On the other hand, including components from MHSA, such as Lily (qvffn) or Lily (kvffn), improves performance on structured datasets. This phenomenon highlights that fine-tuning should not only consider the method but also the strategic allocation of limited parameter budgets to maximize performance.

Simultaneously, we notice that N_e plays a crucial role in model performance on certain datasets. Varying N_e results in different levels of overlap among HP experts’ specialization layers, which we refer to as the attention granularity. Higher values of N_e lead to more HP experts and, consequently, finer granularity. Conversely, smaller N_e results in coarser granularity. Interestingly, different datasets exhibit optimal N_e values, indicating their preferred granularity. In such cases, simply increasing N_e to add more parameters may not always lead to better performance. We provide a further detailed analysis of this phenomenon in the following section.

Overall, Lily surpasses LoRA and AdaptFormer by a large margin on the VTAB-1K benchmark while requiring fewer configurations of N_e than the number of layers in ViT (for ViT-B used in this experiment, it’s 12). This allows Lily to achieve higher performance with fewer parameters compared to traditional low-rank adaptation methods like LoRA.

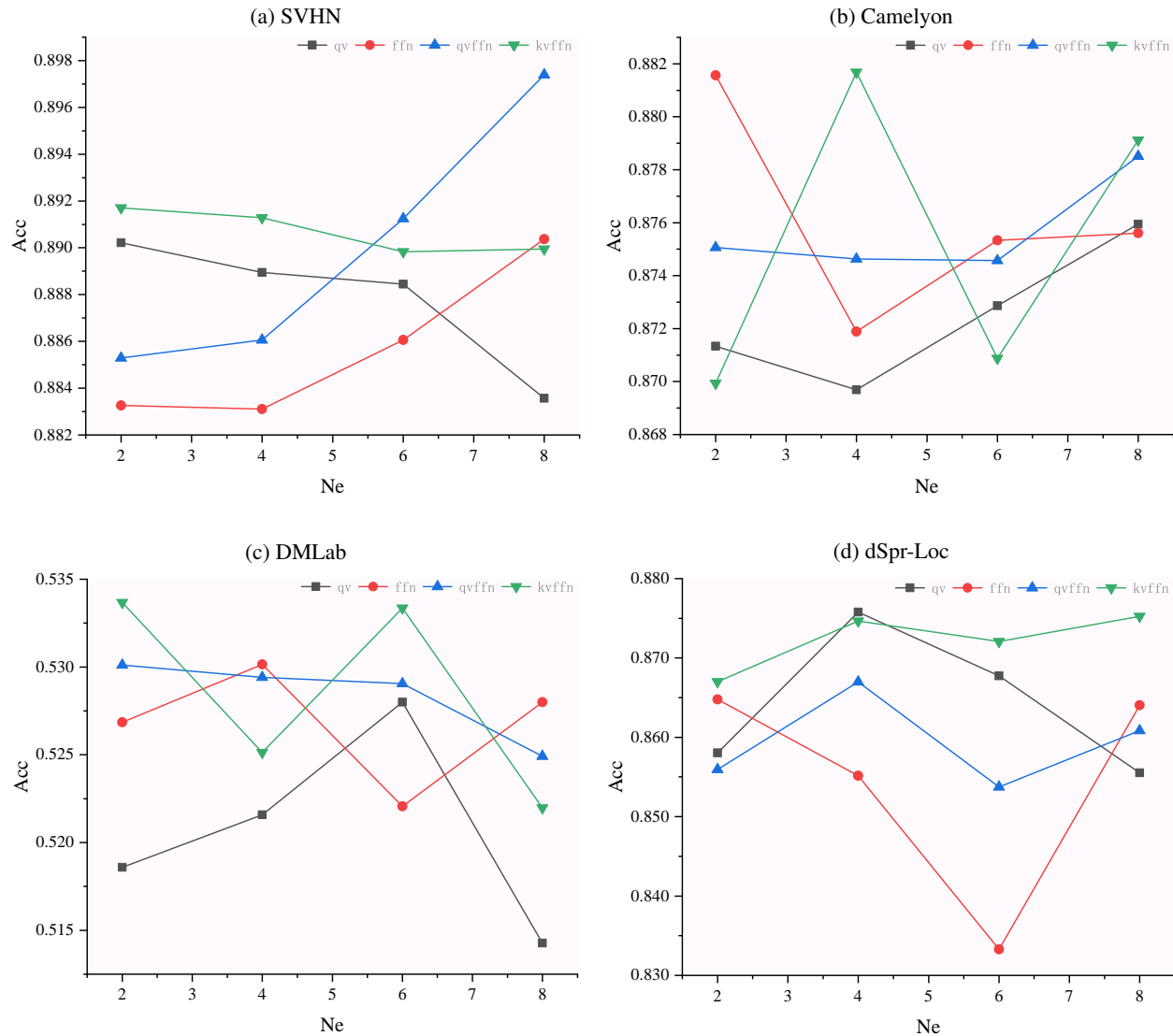


Figure 3: The effect of attention granularity by N_e on 4 datasets in the VTAB-1K benchmark.

4.2.2 Analysis of the attention granularity

As mentioned earlier, we refer to the varying levels of overlap among different HP experts’ specialization ranges’ due to changes in N_e as the attention granularity of Lily. In this section, we provide concrete analysis to illustrate the existence of an optimal granularity for different datasets under different adaptation configurations like employing Lily on the FFN, Lily (ffn), or employing Lily on k, v and ffn, Lily(kvffn). The results are in Figs. 3.

Specifically, in some tasks such as DMLab 3c and dSpr-Loc 3d, we can observe a clear change in attention granularity and performance when using Lily (qv) with different values of N_e . In DMLab, Lily (qv) shows an increasing trend when N_e is less than 6, and increasing N_e also increases the attention granularity and improves performance with a larger number of parameters. However, when N_e is greater than 6, increasing N_e and the number of parameters leads to worse performance. In this case, $N_e = 6$ is the optimal attention granularity for this configuration. Similarly, in dSpr-Loc, the best attention granularity for Lily (qv) is $N_e = 4$ as observed in Fig. 3d.

However, not all configurations follow this trend. In dSpr-Loc, the performance of Lily (ffn) decreases as N_e increases up to 6, but then improves when $N_e = 8$. This performance gain is due to the larger number of parameters enhancing the learning capability, thus offsetting the negative impact of a sub-optimal attention granularity. Similar behavior can

	Natural							Specialized				Structured							Average	Params(M)	
	Cifar100	Caltech101	DTD	Flowers102	Pets	SVHN	Sun397	Camelyon	EuroSAT	Resisc45	Retinopathy	Clec-Count	Clec-Dist	DMLab	KITTT-Dist	dSpr-Loc	dSpr-Ori	sNORB-Azim			sNORB-Ele
<i>Traditional Fine-Tuning</i>																					
Full Vim	47.7	89.4	64.2	89.0	87.7	90.6	35.1	84.5	93.9	81.0	74.5	67.5	52.9	47.3	78.9	75.3	53.9	33.3	29.4	70.1	26
Full ViT	49.4	89.3	65.5	91.7	89.1	91.4	33.5	85.9	93.6	85.4	74.3	54.7	55.2	48.7	79.7	68.2	49.7	31.5	27.7	69.9	86
Linear Mamba	40.9	83.3	57.3	66.3	86.3	38.4	34.6	79.0	87.6	65.0	73.6	36.3	35.1	33.3	64.8	23.0	21.6	15.1	21.7	55.3	0
Linear ViT	50.6	85.6	61.4	79.5	86.5	40.8	38.0	79.7	91.5	71.7	65.5	41.4	34.4	34.1	55.4	18.1	26.4	16.5	24.8	66.4	0
<i>PETL methods on ViT</i>																					
AdaptFormer	56.2	89.6	67.2	91.2	91.1	85.9	42.1	85.4	94.6	84.0	74.3	75.8	58.6	48.6	79.6	81.6	53.7	29.6	35.2	72.4	0.147
LoRA	56.4	89.0	66.9	91.2	90.4	86.9	41.5	85.4	95.1	84.1	75.2	75.8	61.7	47.7	80.5	80.4	52.0	29.4	35.7	72.5	0.295
<i>Minimal-Parameters Methods</i>																					
DeltaFit ₄	57.6	88.0	64.6	85.7	89.7	85.8	39.8	82.4	92.9	78.7	72.8	77.4	55.8	43.2	79.3	73.1	51.2	27.4	33.0	69.9	0.019
DeltaFit ₈	58.1	88.3	64.6	85.8	89.8	87.5	39.4	83.0	93.3	78.7	72.6	78.2	57.7	43.9	78.6	76.3	51.9	29.3	33.6	70.5	0.038
DeltaInFit	57.3	88.7	66.8	87.4	90.5	86.4	40.4	82.4	93.7	80.8	73.5	80.4	55.9	44.4	79.7	73.7	53.1	30.5	31.7	70.9	0.057
Lily _{≤6} ^{4,4}	58.2	88.5	65.6	87.1	90.7	87.5	40.4	83.3	94.1	79.7	73.8	81.2	57.3	44.1	80.9	79.3	54.1	30.0	33.7	71.4	0.074
<i>High-Performance Methods</i>																					
Lily ₅ ^{4,8}	57.8	89.0	66.2	87.8	90.5	87.0	40.5	83.0	94.1	80.1	73.3	81.6	57.8	45.0	81.0	80.1	54.5	32.1	33.1	71.6	0.146
Lily _{≤4} ^{8,8}	58.0	89.1	66.3	87.7	90.9	87.7	40.3	83.2	94.1	80.8	74.7	82.1	58.4	44.9	80.3	80.7	53.9	30.2	34.6	71.9	0.133
Lily _{≤17} ^{4,8}	57.8	89.4	66.2	87.8	90.5	88.1	40.5	84.1	94.3	81.3	75.1	81.6	57.8	46.5	81.0	82.9	55.2	32.1	34.8	72.3	0.196

Table 2: Full results of Lily on Vim-s on the VTAB-1K benchmark. Averages are calculated based on the averages within each group. * denotes results of linear probing on ViT is from [24]. Green signifies the best performance on the tasks.

be observed in configurations such as Camelyon 3b with Lily (ffn), Lily (qv), and Lily (kvffn), and dSpr-Loc 3d with Lily (qvffn).

In contrast, the performance curves of configurations in the SVHN 3a are mostly monotonic. The monotonic increasing curves of Lily (ffn) and Lily (qvffn) is due to the positive impact of additional parameters and increased attention granularity. On the other hand, the monotonic decreasing curves illustrate the impact of attention granularity: having more parameters does not always lead to better performance, the actual optimal attention granularity is what needed to achieve the best performance.

In summary, by analyzing the effects of attention granularity on Lily in different configurations across various tasks and model adaptation positions, we observed an interesting phenomenon in the trade-offs between parameters and performance in PETL research: simply increasing N_e to achieve larger attention granularity and more parameters does not necessarily lead to performance gains. Sometimes, a more suitable configuration with a smaller N_e can ultimately result in optimal performance.

4.3 Lily on Mamba

Regarding the Mamba architecture, we also evaluate Lily on the VTAB-1K benchmark for its credibility at assessing the effectiveness of fine-tuning methods.

We compare Lily to traditional fine-tuning which includes full fine-tuning and linear probing on both ViT and Vision Mamba (Vim) to investigate each model’s pros and cons. Concurrently, we also apply LoRA and AdaptFormer, which are among the state-of-the-art methods for ViT, to provide a comparative analysis with our proposed approach. Meanwhile, we also propose two methods to adapt Mamba with weight sharing only for a comprehensive comparison: DeltaFit uses the hierarchical structure introduced in Lily for Δ , but sets N_e to 1, thus eliminating the need for a router. For the input projection, DeltaFit employs a pair of model-shared LP and HP. The other method, DeltaInFit, uses the hierarchical structure with N_e set to 1 for both Δ and the input projection.

The hidden dimension d is set to both 4 and 8 for DeltaFit₄ and DeltaFit₈ respectively. For DeltaInFit, in order to control the number of parameters as much as possible, we set the d of input projections as small as merely 1 and the d of Δ to 4. Lily_{≤r}^{m,n} denotes that for Δ , d is set to m , and for input projections, d is assigned n . The notation $\leq r$ signifies that the number of parameters, N_e , is searched within a range less than or equal to r . Conversely, Lily_r indicates that N_e is precisely r . For Lily_{≤6}^{4,4}, Lily_{≤4}^{8,8} and Lily_{≤17}^{4,8}, N_e is searched in $\{3, 6\}$, $\{2, 4\}$ and $\{5, 6, 17\}$ respectively.

When considering the number of parameters, we only take into account the parameters within the backbone and exclude the parameters in the classification head. For backbone of Vim and ViT, we use Vim-S [34] and ViT-B/16 [8] pretrained on supervised ImageNet-1K [7]. For experimental settings, we use AdamW [18] as the optimizer and a cosine learning-rate scheduler. In DeltaFit and DeltaInFit we utilize bias in the projector while in Lily we don't. We use a batchsize of 64. For results of the proposed methods, we position them within two spectrums, ranging from the most parameter-efficient approach to the best-performing one. We categorize DeltaFit, DeltaInFit, and $Lily_{\leq 6}^{4,4}$ under the most parameter-efficient group, as they utilize fewer than 0.1M parameters. Meanwhile, $Lily_{\leq 4}^{8,8}$, $Lily_{\leq 5}^{4,8}$, and $Lily_{\leq 17}^{4,8}$ are placed in the best-performing category since they surpass the ViT full-fine-tuning baseline by more than 1.5 points, despite using slightly more parameters.

The results are shown in Table 2 and from which we can observe that our methods surpasses the full fine-tuning and linear probing baselines in both parameter efficiency and performance. Our most parameter-efficient methods only utilizes 0.037M, 0.058M and 0.074M parameters, achieving a remarkable 650-fold, 433-fold and 351-fold reduction of parameters compared to full fine-tuning, which requires 26M parameters. Our best-performing methods $Lily_{\leq 17}^{4,8}$ surpass the baseline by a significant margin of 2.2 points, which is a remarkable achievement considering its small number of parameters. Specifically, ΔFit_4 can also perform quite well even when only 0.02M parameters are being updated. ΔFit_8 surpasses the baseline by 0.4 points, while $\Delta InFit$ surpasses the baseline by 0.8 points. Among all the methods explored, Lily strikes the best balance between parameter efficiency and performance. $Lily_{\leq 6}^{4,4}$ surpass the baseline by 1.3 points while only updating 0.074M parameters. $Lily_{\leq 5}^{4,8}$ and $Lily_{\leq 4}^{8,8}$ perform quite well, trading off between parameters and performance. $Lily_{\leq 17}^{4,8}$ is the best performing method which achieves 72.3 while only utilizing 0.196M parameters.

Additionally, we compare the performance of ViT and Vim models. Overall, both models exhibit similar performance when fully fine-tuned. ViT with LoRA and AdaptFormer achieves impressive results, outperforming DeltaFit and DeltaInFit, which solely rely on the hierarchical structure. However, by employing Lily, we attain performance comparable to LoRA and AdaptFormer on ViT. Upon closer inspection, Vim demonstrates significant strengths on specific datasets like SVHN, Cifar100, and Clecr-Count, whereas ViT excels on datasets such as Resisc45 and Flowers102. These observations highlight the unique capabilities of each model, validating the potential of a hybrid approach that combines both models as a promising future study direction to leverage their respective advantages.

Overall, our approach achieves a good balance between the number of parameters and performance, attaining the best results on 14 out of 19 tasks in VTAB-1K in all Mamba-based PETL methods with a extremely small number of parameters. Our method leverages the parameters in SSM, demonstrating the usefulness of adaptation with the selective S6 model. One current research trend focuses on reinventing recurrent networks or employing linear attention as the next generation of foundation models. As the use of foundation models is inseparable from the need for efficient adaptation, our method paves the way for future investigations into whether this class of models has the potential to replace transformers.

4.4 Visualization of the adptive nature of Lily

One of the distinctive features of Lily is its ability to allocate unique set of weights of experts for different layers depending on the characteristics of the layer where inputs are, termed as the adptive nature. This allows it to focus on specific experts and achieve targeted adaptation of the input. Here, we visualize the cumulative sum of all the weights allocated to each layer type: layer 2, 13, and 22, after fine-tuning for 30 epochs on nine datasets. We choose layer 2, 13, and 22 to represent shallow, middle, and deep layer types, respectively, and showcase their assigned weights from Figures in 4 to illustrate the nature of targeted adaptation.

As observed in the figures, while not always in a one-to-one manner, many experts exhibit high weights for specific layer types while remaining inactive in others. For instance, in Retinopathy, Cifar100, and EuroSAT, HP_3 , HP_2 , and HP_3 , respectively, show significantly higher activity for the middle layer compared to other experts. For deeper layers, HP_2 dominates in KITTI-Dist, while HP_2 takes the lead in Flowers102. For shallow layers, HP_1 is mainly active in Camelyon, while the activities of different experts are not significantly varied across other datasets.

Therefore, we find that the process of selective weights allocation in Lily not only targets different layers within the same dataset but also automatically learns how to allocate weights for different datasets based on their unique characteristics. This further highlights the advantages of our method in multi-task fine-tuning scenarios.

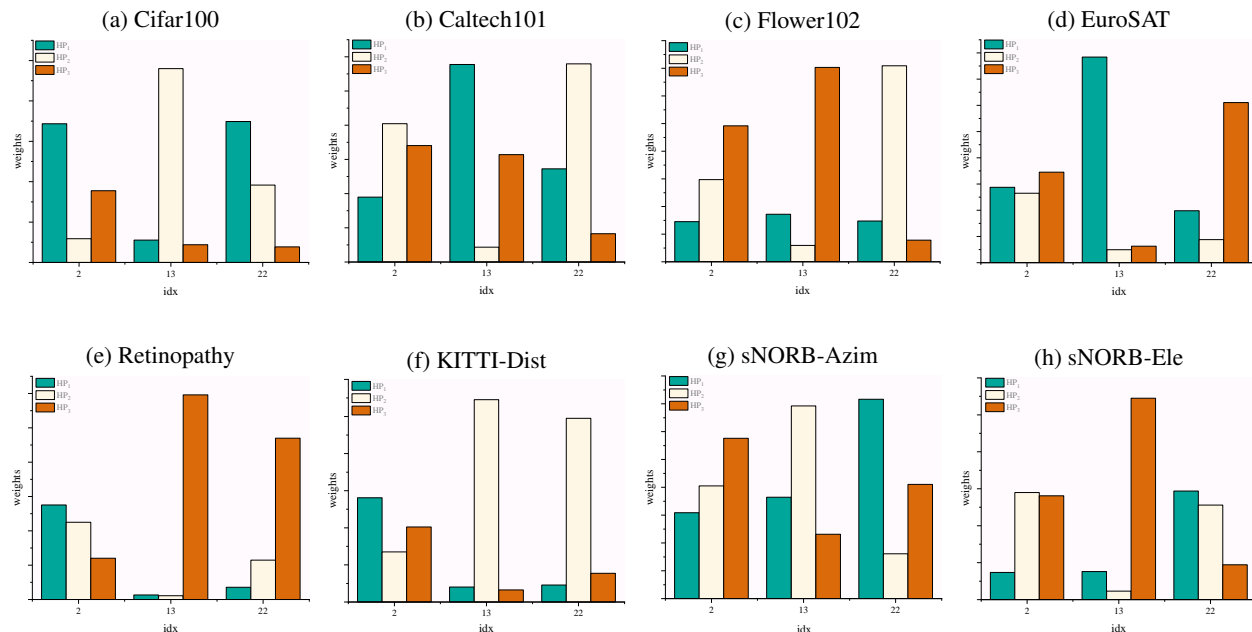


Figure 4: An visualization of the process of selective weights allocation in Lily. Here we choose 8 tasks out of 19 in the VTAB-1k benchmark to give a comprehensive analysis.

4.5 Ablation Study

In this section, we analyze some key mechanisms of Lily. We examine the effect of the adaptive nature brought by the router on the overall performance under the Transformer. On Mamba, we analyze the effects of the hierarchical structure employed in Lily.

To test the validity of the routers, we still maintain the hierarchical structure but bypass the router by directly summing the outputs of all experts to obtain the combined HP, denoted as Lily (monoscale) in Table 3. To validate the effectiveness of the hierarchical structure, we use the basic LoRA adapter setting for both the Δ and input projections of Lily on Mamba, denoted as Lily₀^{4,4}.

Method	Average	Natural	Specialized	Structured
Lily (ffn)	76.84	82.1	86.3	62.2
Lily (ffn monoscale)	76.58	81.8	86.0	62.0
Lily (kvffn)	77.28	82.2	86.2	63.4
Lily (kvffn monoscale)	77.10	82.1	86.0	63.2

Method	Average	Natural	Specialized	Structured	Params(M)
Lily ₃ ^{4,4}	71.05	73.9	82.4	56.8	0.066
Lily ₀ ^{4,4}	70.06	73.0	82.0	55.2	0.053

Table 3: Ablation on effects of the router and the hierarchical structure proposed by Lily.

The results of the ablations are presented in 3. The experimental results demonstrate the effectiveness of Lily’s monoscale mode on Transformers, outperforming LoRA by a significant margin. This success is attributed to Lily’s proposed hierarchical structure, which allows for the utilization of information from all layers, resulting in a comprehensive adaptation. Furthermore, by incorporating a router to dynamically allocate weights to experts, we achieve notable performance gains with extremely minimal additional parameters ($d \times N_e$, where $d = 16$ and $N_e = 3$ result in only 48 additional parameters). The superiority of our hierarchical structure is further validated through experiments on Mamba, where we compare it to a vanilla adapter that does not employ the hierarchical architecture.

In summary, our experiments confirm the efficacy of Lily’s hierarchical structure, enabling the model to consider information from multiple layers during adaptation. The addition of a router for dynamic weight allocation, coupled with minimal parameter increases, underscores the effectiveness of Lily’s attention-like mechanism of selective weights allocation, leading to notable performance enhancements.

5 Conclusion

In this paper, we introduce a novel low-rank adaptation framework named **Low-rank interconnected adaptation across layers (Lily)**. Lily operates within a hierarchical structure that we propose, where low-dimension projectors (LPs) responsible for projecting inputs to a low-dimensional space are fixed and layer-specific, positioned at the bottom of the hierarchy. Conversely, high-dimension projectors (HPs), tasked with restoring the dimension, are decoupled from specific layers and form a shared global HP module at the top of the hierarchy. This hierarchical arrangement enables comprehensive adaptation by allowing access to information from all layers when adapting each individual layer. Treating the HPs in the global HP as experts specialized in feature learning for different layers, we employ a router to selectively allocate weights to these experts, tailoring their contributions to the unique characteristics of each layer. Experiments validate that Lily achieves comparable or superior performance with a reduced parameter count, striking a good balance between parameter efficiency and performance.

References

- [1] Amjad Almahairi et al. “Dynamic capacity networks”. In: *International Conference on Machine Learning*. PMLR. 2016, pp. 2549–2558.
- [2] Maximilian Beck et al. “xLSTM: Extended Long Short-Term Memory”. In: *arXiv preprint arXiv:2405.04517* (2024).
- [3] Yoshua Bengio, Nicholas Léonard, and Aaron Courville. “Estimating or propagating gradients through stochastic neurons for conditional computation”. In: *arXiv preprint arXiv:1308.3432* (2013).
- [4] Dan Biderman et al. “Lora learns less and forgets less”. In: *arXiv preprint arXiv:2405.09673* (2024).
- [5] Shoufa Chen et al. “Adaptformer: Adapting vision transformers for scalable visual recognition”. In: *Advances in Neural Information Processing Systems* 35 (2022), pp. 16664–16678.
- [6] Andrew Davis and Itamar Arel. “Low-rank approximations for conditional feedforward computation in deep neural networks”. In: *arXiv preprint arXiv:1312.4461* (2013).
- [7] Jia Deng et al. “Imagenet: A large-scale hierarchical image database”. In: *2009 IEEE conference on computer vision and pattern recognition*. Ieee. 2009, pp. 248–255.
- [8] Alexey Dosovitskiy et al. “An image is worth 16x16 words: Transformers for image recognition at scale”. In: *arXiv preprint arXiv:2010.11929* (2020).
- [9] David Eigen, Marc’Aurelio Ranzato, and Ilya Sutskever. “Learning factored representations in a deep mixture of experts”. In: *arXiv preprint arXiv:1312.4314* (2013).
- [10] Chongyang Gao et al. “Higher Layers Need More LoRA Experts”. In: *arXiv preprint arXiv:2402.08562* (2024).
- [11] Albert Gu and Tri Dao. “Mamba: Linear-time sequence modeling with selective state spaces”. In: *arXiv preprint arXiv:2312.00752* (2023).
- [12] Sepp Hochreiter and Jürgen Schmidhuber. “Long short-term memory”. In: *Neural computation* 9.8 (1997), pp. 1735–1780.
- [13] Neil Houlsby et al. “Parameter-efficient transfer learning for NLP”. In: *International conference on machine learning*. PMLR. 2019, pp. 2790–2799.
- [14] Edward J Hu et al. “Lora: Low-rank adaptation of large language models”. In: *arXiv preprint arXiv:2106.09685* (2021).
- [15] Shibo Jie and Zhi-Hong Deng. “Fact: Factor-tuning for lightweight adaptation on vision transformer”. In: *Proceedings of the AAAI Conference on Artificial Intelligence*. Vol. 37. 1. 2023, pp. 1060–1068.
- [16] Angelos Katharopoulos et al. “Transformers are rnns: Fast autoregressive transformers with linear attention”. In: *International conference on machine learning*. PMLR. 2020, pp. 5156–5165.
- [17] Yann LeCun, Koray Kavukcuoglu, and Clément Farabet. “Convolutional networks and applications in vision”. In: *Proceedings of 2010 IEEE international symposium on circuits and systems*. IEEE. 2010, pp. 253–256.
- [18] Ilya Loshchilov and Frank Hutter. “Decoupled weight decay regularization”. In: *arXiv preprint arXiv:1711.05101* (2017).
- [19] Roy Miles et al. “VeLoRA: Memory Efficient Training using Rank-1 Sub-Token Projections”. In: *arXiv preprint arXiv:2405.17991* (2024).
- [20] Bo Peng et al. “Rwkv: Reinventing rnns for the transformer era”. In: *arXiv preprint arXiv:2305.13048* (2023).
- [21] Jonas Pfeiffer et al. “Adapterfusion: Non-destructive task composition for transfer learning”. In: *arXiv preprint arXiv:2005.00247* (2020).

- [22] Olaf Ronneberger, Philipp Fischer, and Thomas Brox. “U-net: Convolutional networks for biomedical image segmentation”. In: *Medical image computing and computer-assisted intervention—MICCAI 2015: 18th international conference, Munich, Germany, October 5-9, 2015, proceedings, part III 18*. Springer. 2015, pp. 234–241.
- [23] Noam Shazeer et al. “Outrageously large neural networks: The sparsely-gated mixture-of-experts layer”. In: *arXiv preprint arXiv:1701.06538* (2017).
- [24] Cheng-Hao Tu, Zheda Mai, and Wei-Lun Chao. “Visual query tuning: Towards effective usage of intermediate representations for parameter and memory efficient transfer learning”. In: *Proceedings of the IEEE/CVF Conference on Computer Vision and Pattern Recognition*. 2023, pp. 7725–7735.
- [25] Cheng-Hao Tu, Zheda Mai, and Wei-Lun Chao. “Visual query tuning: Towards effective usage of intermediate representations for parameter and memory efficient transfer learning”. In: *Proceedings of the IEEE/CVF Conference on Computer Vision and Pattern Recognition*. 2023, pp. 7725–7735.
- [26] Ashish Vaswani et al. “Attention is all you need”. In: *Advances in neural information processing systems 30* (2017).
- [27] Elena Voita, Rico Sennrich, and Ivan Titov. “The bottom-up evolution of representations in the transformer: A study with machine translation and language modeling objectives”. In: *arXiv preprint arXiv:1909.01380* (2019).
- [28] Taiqiang Wu et al. “Mixture-of-Subspaces in Low-Rank Adaptation”. In: (2024). URL: arxiv.org/abs/2406.11909.
- [29] Ted Zadouri et al. “Pushing mixture of experts to the limit: Extremely parameter efficient moe for instruction tuning”. In: *arXiv preprint arXiv:2309.05444* (2023).
- [30] Xiaohua Zhai et al. “The visual task adaptation benchmark”. In: (2019).
- [31] Qingru Zhang et al. “Adaptive budget allocation for parameter-efficient fine-tuning”. In: *International Conference on Learning Representations*. Openreview. 2023.
- [32] Zihan Zhong et al. “Convolution Meets LoRA: Parameter Efficient Finetuning for Segment Anything Model”. In: *arXiv preprint arXiv:2401.17868* (2024).
- [33] Zongwei Zhou et al. “Unet++: A nested u-net architecture for medical image segmentation”. In: *Deep Learning in Medical Image Analysis and Multimodal Learning for Clinical Decision Support: 4th International Workshop, DLMIA 2018, and 8th International Workshop, ML-CDS 2018, Held in Conjunction with MICCAI 2018, Granada, Spain, September 20, 2018, Proceedings 4*. Springer. 2018, pp. 3–11.
- [34] Lianghui Zhu et al. “Vision mamba: Efficient visual representation learning with bidirectional state space model”. In: *arXiv preprint arXiv:2401.09417* (2024).
- [35] Barret Zoph et al. “St-moe: Designing stable and transferable sparse expert models”. In: *arXiv preprint arXiv:2202.08906* (2022).

6 Appendix